Stability of a laminar boundary layer flowing along a concave surface with uniform mainstream velocity

K. H. Yeo, A. Brown and B. W. Martin*

Predictions, by the Galerkin method, are presented of the stability of three-dimensional disturbances in laminar boundary-layer flow at zero pressure gradient along a concave surface. The analysis confirms Meksyn's finding[1] of more than one critical state; predictions for the first agree with those of Kahawita and Meroney[2] at low Goertler number G and with the vortex amplification predictions of Smith[3] at high G. Both the first and second critical states have G values below those of Meksyn; the amplification field of the second, however, encompasses the range of available measurements, and therein, has dimensionless vortex energy levels only half those of the first. The plausibility of least vortex energy as a determining factor in favour of the second critical field is further strengthened by its limited G range, the upper limit of about 7 corresponding closely to Liepmann's observations[4,5] of the onset of transition to turbulence. These findings are almost insensitive to mainstream Mach numbers up to 0.9, stagnation conditions up to 15 bar and 1200 K, and Reynolds numbers from 2000 to 6000 based on boundary layer thickness

Keywords: *turbine blades, vortices, boundary layers*

This paper is prompted by the probability of the development of Taylor–Goertler vortices in laminar boundary-layer flow over the concave pressure surfaces of gas-turbine stator and rotor blades. Such longitudinal vortices, first predicted by Goertler[6] and illustrated in Fig 1, are formed by the instability that occurs when the centrifugal forces acting on the fluid outweigh the ability of the radial pressure gradient and viscous forces to damp out small disturbances.

In the light of the boundary-layer measurements of Liepmann[5] and the heat-transfer measurements of McCormack, Welker and Kelleher[7] in low-speed flow over concave surfaces, Martin and Brown[8] suggested that Taylor–Goertler vorticity, when interacting with mainstream turbulence, might account for cascade measurements of heat transfer on blade pressure surfaces greater than for a laminar boundary layer on a flat plate. They hypothesized that the marked chordwise fluctuations in local heat transfer prior to transition arose from the progressive shedding of paired opposed vortices over a given blade span due to increases in vortex wavelength λ with increases in $\beta\theta Re_\theta$ (where β is the amplification rate) in the flow direction. This possibility may require review in the light of what follows.

More recent detailed examination of flow and heat-transfer measurements by Brown and Martin[9] indicates only limited influence of the interaction between vorticity and mainstream turbulence in enhancing laminar boundary-layer heat transfer. This study further suggests that transition to a turbulent boundary layer could be inhibited by keeping the velocity gradient factor k in excess of the laminarization value of 2.5×10^{-6} first obtained by Launder[10]. Maintaining entirely laminar flow, albeit with vorticity and mainstream turbulence, over the pressure surface of a high-temperature turbine blade by a sufficiently strong favourable pressure gradient would give lower heat transfer to the blade than if transition occurred. The advantages of blade design based on this criterion would thus include fuel economy through the ability to operate at higher turbine inlet temperatures or by mitigating blade-cooling problems. Brown and Martin found that this criterion also yields improved performance compared to conventional blade design, for trailing-edge mainstream

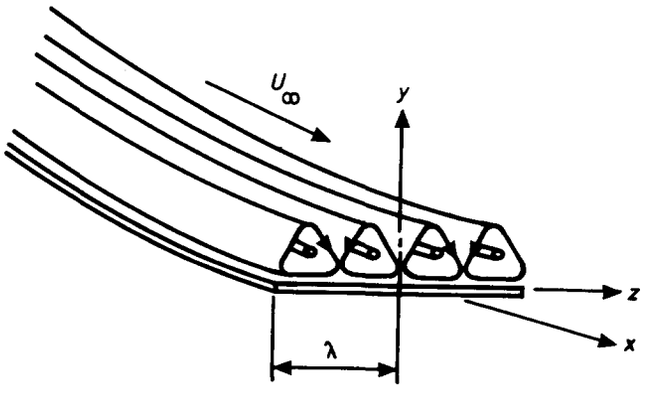

Fig 1 Taylor–Goertler vortices on a concave surface

* Department of Mechanical Engineering and Engineering Production, University of Wales Institute of Science and Technology, Cardiff, UK
Received 30 September 1983 and accepted for publication on 19 March 1984

 0142–727X/84/020067–13$03.00

Mach number M_∞ between 0.5 and 1.0, through increased blade lift and reduced aerodynamic drag.

Reliable knowledge is required, therefore, of Goertler vortices in high-temperature compressible flow with strongly-favourable pressure gradients in a laminar boundary layer along concave surfaces of varying curvature, and of the extent to which such secondary flows, with mainstream turbulence, enhances laminar heat transfer. For these conditions we need ultimately to predict both neutral stability and the relation between Goertler number G and $\alpha\theta$ (where α is wave number) with variation in $\beta\theta Re_\theta$ in the downstream direction x along the concave surface. To date this has not been established theoretically, even for the simple Blasius flow assumed in most investigations, in a way which, for instance, convincingly predicts the measurements of Tani[11] and Tani and Sakagami[12].

By analysis of a small three-dimensional time-dependent disturbance superimposed on the Blasius boundary layer, Goertler[6] found that the neutral stability condition, or critical state for zero β, achieved

Nomenclature

A	Dimensionless product, $\alpha\delta = 2\pi\delta/\lambda$
a_i	Coefficients in Eqs (23)–(26) for $i = 1$ to 24
B	Dimensionless amplification factor $\beta\delta$
d	Function of M and k' defined in Eq (16)
E	Dimensionless decay factor in Eqs (23)–(26)
E_a	Total energy of boundary-layer flow in the presence of vortices
E_b	Total energy of boundary-layer flow in the absence of vortices
E_v	Energy of vortices, $(E_a - E_b)$
$F_j(k')$	Universal functions of k', where j = 1 to 4
G	Dimensionless Goertler number, $\mathrm{Re}_\theta(\theta/r)^{1/2}$
K	Dimensionless product, $\kappa\delta = \delta/r$
k	Velocity gradient factor, $(\nu/U_\infty^2)\,\mathrm{d}U_\infty/\mathrm{d}x$
k'	Function of M and Λ defined in Eq (17)
M	Mach number
n	Energy multiplier or polytropic index
P	Square matrix whose elements are functions of η
p	Absolute pressure
$\hat{p}$	Perturbed pressure component relative to mainstream dynamic head, $p_1/(\frac{1}{2}\rho_\infty U_\infty^2)$
Pr	Fluid Prandtl number
Q	Square matrix whose elements are functions of η
R	Gas constant
r	Radius of curvature of concave pressure surface
Re_δ	Reynolds number based on boundary-layer thickness, $U_\infty\delta/\nu_\infty$
Re_θ	Momentum-thickness Reynolds number, $U_\infty\theta/\nu_\infty$
Re_x	Length Reynolds number, $U_\infty x/\nu_\infty$
s	Length of concave pressure surface
T	Temperature
U_∞	Mainstream velocity in x-direction
U'_∞/U_∞	Mainstream turbulence intensity
$\hat{U}$	Unperturbed velocity component in x-direction relative to mainstream velocity, u_0/U_∞
u	Velocity component in x-direction
$\hat{u}$	Perturbed velocity component in x-direction relative to mainstream velocity, u_1/U_∞
$\hat{V}$	Unperturbed velocity component in y-direction relative to mainstream velocity, v_0/U_∞
v	Velocity component in y-direction
$\hat{v}$	Perturbed velocity component in y-direction relative to mainstream velocity, v_1/U_∞
w	Velocity component in z-direction
$\hat{w}$	Perturbed velocity component in z-direction relative to mainstream velocity, w_1/U_∞
x	Distance downstream along concave surface
y	Distance from concave surface normal to surface
z	Distance along concave surface normal to flow direction
α	Wave number, $2\pi/\lambda$
β	Rate of amplification of vortices
γ	Ratio of gaseous specific heats
δ	Boundary-layer thickness
ε	Distance along surface relative to surface length, x/s
η	Distance normal to surface relative to boundary-layer thickness, y/δ
θ	Boundary-layer momentum thickness
κ	Curvature of concave surface $1/r$
Λ	Modified Pohlhausen parameter, $(\theta^2/\nu)/(\mathrm{d}U_\infty/\mathrm{d}x)$
λ	Vortex wavelength $2\pi/\alpha$
μ	Dynamic viscosity of fluid
$\hat{\mu}_0$	Boundary-layer viscosity relative to mainstream viscosity, μ_0/μ_∞
ν	Kinematic viscosity
π_v	Dimensionless vortex energy defined by Eq (36)
ρ	Density of fluid
$\hat{\rho}$	Perturbed density component relative to mainstream density, ρ_1/ρ_∞
$\hat{\rho}_0$	Unperturbed density component relative to mainstream density, ρ_0/ρ_∞
ψ	Stream function
ω	Error in Galerkin representation

Superscripts and subscripts

$\hat{}$	Dimensionless ratio
∞	Mainstream condition
0	Unperturbed component in boundary layer
1	Perturbed component in boundary layer
x	Based on distance along concave surface
θ	Based on boundary-layer momentum thickness
w	Denotes condition at concave surface

minimum G of 0.58 at $\alpha\theta = 0.14$. Larger $\beta\theta Re_\theta$ yielded similar curves with minima at increasing $\alpha\theta$ and correspondingly higher G. Vortex disturbances have since been assumed to originate at minimum G, thereby determining their initial wavelength. Meksyn's solution[1] of the same equations of motion by an asymptotic method, rather than by transformation, indicated multiple critical states, the first (I) with minimum G of 3.65 at $\alpha\theta = 0.4$, and the second (II) with minimum G of 10.7 at $\alpha\theta = 0.75$. Using alternative procedures to solve Goertler's stability equations, Hammerlin's neutral stability prediction[13], though closer to Goertler's than Meksyn's, becomes rather flat at around $G = 0.3$ for $\alpha\theta < 0.05$, so that minimum G is attained only when $\alpha\theta = 0$, and λ for the initial vortex disturbance is infinite. These are among the predictions shown in Fig 2.

Smith[3] analysed Blasius flow by the Galerkin method, assuming distance-dependent disturbances to be more consistent with physical reality than time-dependent disturbances, an argument accepted in all subsequent treatments. Smith also included in his simplified equations certain terms involving velocities in the growing boundary layer normal to the concave surface and certain higher-order terms describing the effects of surface curvature on the disturbances. These previously neglected terms were based on order-of-magnitude analysis which, on re-examination, leaves room for doubt in the justification for his choice, even for his assumed range of variables. While for large $\alpha\theta$ Smith's neutral stability curve is comparable with that of Hammerlin, it gives minimum G of 0.31 around $\alpha\theta = 0.07$ (Fig 2) and hence finite initial λ. Smith also presented curves of constant $\beta\theta Re_\theta$ up to 100, with corresponding increases in $\alpha\theta$ for minimum G, but cautions that the central portions may have errors up to 10% and the extremities even more.

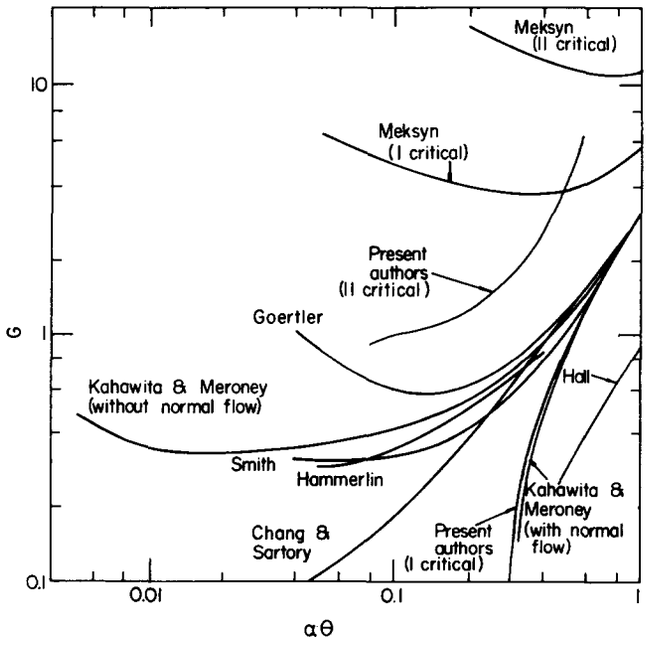

Fig 2 Previous and present predictions of marginal stability of Taylor–Goertler vortices

The differential equations solved by numerical integration by Chang and Sartory[14] as the limiting case of their MHD study are those solved by Hammerlin except for the inclusion of terms involving the normal velocity component of the Blasius flow, but without the higher-order curvature terms which Smith regarded as equally important. Chang and Sartory found (Fig 2) that both minimum G and the corresponding $\alpha\theta$ for neutral stability tended to zero; they hence surmised that at low $\alpha\theta$ the neglected curvature terms might well limit the degree of instability and hence the vortex size below infinity, though they suspect that in this region Smith's predictions of G could be at least an order of magnitude too large.

These views are supported by the predictions of Kahawita and Meroney[2], using essentially the same procedure, for the limiting isothermal case of their study of heating effects on Taylor–Goertler vortices in laminar boundary layers. With both normal flow and additional curvature terms retained in the equations, G approaches a zero minimum of neutral stability, as found by Chang and Sartory, but at an asymptote of $\alpha\theta = 0.3$ rather than zero (Fig 2). Smaller $\alpha\theta$ failed to give convergence to a definite positive eigenvalue. The discrepancy with Smith's predictions is ascribed to the latter's use of the Galerkin method combined with an assumed exponential decay rate of dubious validity. Kahawita and Meroney's equations differ from Smith's simplified equations in retaining further curvature terms in each momentum equation, whose effects may also contribute to the discrepancy. Moreover, for $\beta\theta Re_\theta = 0.11$, their minimum G of 0.16 at $\alpha\theta = 0.12$ takes the form of a cusp.

With normal flow terms excluded but curvature terms retained, the neutral stability prediction of Kahawita and Meroney in Fig 2 shows minimum G similar to those of Hammerlin and Smith of about 0.3 but for $\alpha\theta = 0.015$. This discrepancy with Smith's critical $\alpha\theta$ is attributed by Kahawita and Meroney to the further curvature terms in their equations. While they explain how the normal velocity component alters the extent of mainstream penetration of the vortices and in turn the dissipative influence of viscosity in the boundary layer on the perturbations, it is far from clear from their paper which normal flow terms they exclude, whether these cover normal flow derivatives, and whether their choice had regard to Smith's order-of-magnitude analysis.

Hall[15] suggested that the wide disagreement between calculations at small $\alpha\theta$ is due to the effect of boundary-layer growth and that parallel-flow approximations are only valid at large $\alpha\theta$. For this region he developed an asymptotic expansion of the appropriate partial differential linear stability equations when λ for the imposed disturbance is small compared to boundary-layer thickness. Although in qualitative agreement, his neutral stability curve lies significantly below those of Smith and other workers (Fig 2). More recently, Hall[16] described the regime for which his asymptotic results are valid; a vortex of fixed λ is locally unstable for only a finite distance along the boundary layer for surfaces of constant curvature κ. In the absence of non-linear effects, any vortex motion then ultimately decays to zero, but if κ increases at a sufficient rate stability is never

achieved and the vortex flow remains unstable in the x-direction from the location of its inception. Hall's definition of neutral stability is in terms of a dimensionless energy function for the flow, calculated as a function of x, reaching a maximum or minimum.

Aihara[17] and Kobayashi and Kohama[18] analysed by iterative procedure the stability of compressible Blasius flow; the latter workers took account of both density and viscosity changes with temperature in the boundary layer. Because normal flow terms were neglected, their neutral stability curves resemble that of Kahawita and Meroney with that exclusion. For both isothermal and insulated walls, Kobayashi and Kohama find that boundary-layer stability increases somewhat with M_∞, minimum G increasing from 0.56 to 0.6 as M_∞ increases from zero to 0.5 for the insulated wall case. They argue that the destabilising effect of positive density gradient is more than offset by increased boundary-layer viscosity, whose variation was neglected by Aihara and is presumed to account for his numerically different predictions.

Apart from the disagreement between calculations outlined above, there is an evident risk to accurate prediction in neglecting particular terms in the continuity and momentum equations when the associated ranges of the many variables involved cannot be specified sufficiently closely. Accordingly, as part of a longer-term programme relating to high-temperature turbine blades, this paper presents stability calculations for Blasius flow by the Galerkin method in which no significant terms are neglected. The search for eigenvalues may be based on A, B or K; the latter is employed here. The analysis is for air between stagnation conditions of 1 and 15 bar and 300 K and 1200 K, $2000 \leq Re_\delta \leq 6000$ and $0.2 \leq M_\infty \leq 0.9$, the latter taking account of density and viscosity changes with temperature, and using the Gruschwitz[19] equations to evaluate properties of the compressible boundary layer. Yeo[20] has shown these equations to give G values within 10% of those in which compressibility is neglected, at least for M_∞ up to 0.7. The concave surface is assumed adiabatic.

While dimensionless stability predictions hardly differ over the above ranges, the analysis confirms Meksyn's finding[1] of more than one critical state, the first two having lower stability limits than he predicts. The first neutral stability curve follows that of Kahawita and Meroney with normal flow and additional curvature terms retained (Fig 2), but the amplification curves tend to larger G for given $\beta\theta Re_\theta$. In Fig 2 the second neutral stability curve has G values from 0.97 to 6.65 over the restricted range $0.07 \leq \alpha\theta \leq 0.53$. Although amplification curves have minima, the curves do not extend above $G = 7$. There is limited evidence of a third critical state.

The superposition of the second critical field on the first appears to render attempts to relate G to $\alpha\theta$ for the downstream development of vortices along a concave surface even more difficult. The fields are in fact distinguished by the second having values of dimensionless vortex energy π_v roughly half those of the first; this criterion involves less computer time for evaluation than the dimensionless energy function used by Hall[16] to identify neutral stability. For the second critical field, curves of constant π_v imply nearly constant λ and correspond with certain measurements by Tani[11], Tani and Sakagami,[12] Winoto and Crane[21] and Yeo[22]; arguably that of Bippes and Goertler[23] and certainly those of Han and Cox[24] also lie within the second critical field using generally accepted expressions for boundary-layer thickness. As in other areas of natural and applied science, the least energy concept thus seems to play a significant part, somewhat unexpectedly to the exclusion of the first critical state.

Liepmann's[4,5] measurements for Blasius flow indicate that boundary-layer transition to turbulence on concave surfaces begins if $G > 7$; this is also the largest minimum for which eigenvalues could be found for the second critical field, perhaps because the basic laminar equations cease to be valid. As a by-product the analysis, therefore, also yields information consistent with the onset of transition. The second critical field also spans the measured transition range $2.3 \leq G \leq 6.1$ determined by Brown and Martin[9] for blade pressure surfaces in cascade at U'_∞/U_∞ up to 0.17 in favourable pressure gradients below the laminarisation value of k.

Prediction procedure

Following the spacewise representation of Smith[3], we assume that the steady laminar boundary-layer flow along the concave surface is perturbed by the development of longitudinal vortices, such that physical quantities in this disturbed flow can be represented as follows:—

$$u(x, y) = u_0(x, y) + u_1(y) \cos \alpha z \exp \int \beta(x)\, dx \quad (1)$$

$$v(x, y) = v_0(x, y) + v_1(y) \cos \alpha z \exp \int \beta(x)\, dx \quad (2)$$

$$w(x, y) = w_1(y) \sin \alpha z \exp \int \beta(x)\, dx \quad (3)$$

$$p(x, y) = p_0(x, y) + p_1(y) \cos \alpha z \exp \int \beta(x)\, dx \quad (4)$$

$$\rho(x, y) = \rho_0(x, y) + \rho_1(y) \cos \alpha z \exp \int \beta(x)\, dx \quad (5)$$

Through the characteristic equation of state for a perfect gas this system of equations (Eqs (1)–(5)) implicitly involves temperature and we adopt Sutherland's expression for the temperature dependence of the viscosity of air, given for the Kelvin temperature scale by:

$$\mu_0 \propto T_0^{3/2}/(T_0 + 114) \quad (6)$$

In so doing, we neglect any perturbed component of viscosity and, as will be seen below, we do not consider the energy equation. The temperature is assumed to be unperturbed.

By the substitutions:

$$A = \alpha\delta = 2\pi\delta/\lambda; \quad B = \beta\delta;$$
$$K = \kappa\delta = \delta/r; \quad \eta = y/\delta \tag{7}$$
$$\hat{U} = u_0/U_\infty; \quad \hat{V} = v_0/U_\infty;$$
$$\hat{u} = u_1/U_\infty; \quad \hat{v} = v_1/U_\infty \tag{8}$$
$$\hat{w} = w_1/U_\infty; \quad \hat{p} = p_1/(\tfrac{1}{2}\rho_\infty U_\infty^2);$$
$$\hat{\mu}_0 = \mu_0/\mu_\infty; \quad \varepsilon = x/s \tag{9}$$
$$\hat{\rho} = \rho_1/\rho_\infty; \quad \hat{\rho}_0 = \rho_0/\rho_\infty; \quad Re_\delta = U_\infty\delta/\nu_\infty \tag{10}$$

the continuity and x, y, and z-momentum equations, following orthogonal transformation to the concave surface shown in Fig 3, and incorporation of Eqs (1)–(5), can be re-written respectively in the dimensionless forms:

$$\frac{B}{[1-K\eta]}\hat{u} + \left\{\frac{\partial[\ln\hat{\rho}_0]}{\partial\eta} - \frac{K}{[1-K\eta]}\right\}\hat{v} + A\hat{w} + \frac{d\hat{v}}{d\eta} + \left\{\frac{\partial\hat{V}}{\partial\eta} + \left[\frac{B\hat{U}-K\hat{V}}{1-K\eta}\right]\right\}\frac{\hat{\rho}}{\hat{\rho}_0} + \frac{\hat{V}}{\hat{\rho}_0}\frac{d\hat{\rho}}{d\eta} = 0 \tag{11}$$

$$\frac{d^2\hat{u}}{d\eta^2} + \left\{\frac{\partial[\ln\hat{\mu}_0]}{\partial\eta} - \frac{K}{[1-K\eta]} - \frac{\nu_\infty}{\nu_0}\hat{V}Re_\delta\right\}\frac{d\hat{u}}{d\eta} + \left\{\frac{\nu_\infty\hat{V}Re_\delta}{\nu_0}\frac{\partial[\ln\hat{\rho}_0]}{\partial\eta} - \frac{K}{[1-K\eta]}\frac{\partial[\ln\hat{\mu}_0]}{\partial\eta} + \frac{4}{3}\frac{B^2}{[1-K\eta]^2} - A^2 - \frac{\nu_\infty}{\nu_0}\frac{B\hat{U}Re_\delta}{[1-K\eta]} + \frac{\nu_\infty}{\nu_0}Re_\delta\frac{\partial\hat{V}}{\partial\eta}\right\}\hat{u} + \left\{\frac{B}{[1-K\eta]}\frac{\partial[\ln\hat{\mu}_0]}{\partial\eta} - \frac{7}{3}\frac{KB}{[1-K\eta]^2} - \frac{\nu_\infty}{\nu_0}Re_\delta\frac{d\hat{U}}{d\eta} + \frac{\nu_\infty}{\nu_0}\frac{K\hat{U}Re_\delta}{[1-K\eta]}\right\}\hat{v} + \frac{B}{3[1-K\eta]}\frac{d\hat{v}}{d\eta} + \frac{AB}{3[1-K\eta]}\hat{w} + \left\{\frac{K\hat{U}\hat{V}}{[1-K\eta]} - \hat{V}\frac{d\hat{U}}{d\eta}\right\}Re_\delta\frac{\nu_\infty}{\nu_0}\frac{\hat{\rho}}{\hat{\rho}_0} = \frac{\nu_\infty\rho_\infty}{\nu_0\rho_0}\frac{B\hat{p}Re_\delta}{2[1-K\eta]} \tag{12}$$

$$\frac{4}{3}\frac{d^2\hat{v}}{d\eta^2} + \left\{\frac{4}{3}\frac{\partial[\ln\hat{\mu}_0]}{\partial\eta} - \frac{4}{3}\frac{K}{[1-K\eta]} - \frac{\nu_\infty}{\nu_0}\hat{V}Re_\delta\right\}\frac{d\hat{v}}{d\eta} + \left\{\frac{B^2}{[1-K\eta]^2} - \frac{4K}{3[1-K\eta]}\frac{\partial[\ln\hat{\mu}_0]}{\partial\eta} - A^2 - \frac{\nu_\infty}{\nu_0}\frac{B\hat{U}Re_\delta}{[1-K\eta]} - \frac{\nu_\infty}{\nu_0}Re_\delta\frac{\partial\hat{V}}{\partial\eta}\right\}\hat{v} + \left\{\frac{7}{3}\frac{KB}{[1-K\eta]^2} - \frac{\nu_\infty\delta Re_\delta}{\nu_0 s[1-K\eta]}\frac{\partial\hat{V}}{\partial\varepsilon} - \frac{2B}{3[1-K\eta]}\frac{\partial[\ln\hat{\mu}_0]}{\partial\eta} - \frac{\nu_\infty}{\nu_0}\frac{2K\hat{U}Re_\delta}{[1-K\eta]}\right\}\hat{u} + \frac{B}{3[1-K\eta]}\frac{d\hat{u}}{d\eta} - \frac{2A}{3}\frac{\partial[\ln\hat{\mu}_0]}{\partial\eta}\hat{w} + \frac{A}{3}\frac{d\hat{w}}{d\eta} - \left\{\frac{K\hat{U}^2}{[1-K\eta]} + \frac{\delta\hat{U}}{s[1-K\eta]}\frac{\partial\hat{V}}{\partial\varepsilon} + \hat{V}\frac{\partial\hat{V}}{\partial\eta}\right\}Re_\delta\frac{\nu_\infty}{\nu_0}\frac{\hat{\rho}}{\hat{\rho}_0} = \frac{\nu_\infty}{\nu_0}\frac{\rho_\infty}{\rho_0}\frac{Re_\delta}{2}\frac{d\hat{p}}{d\eta} \tag{13}$$

$$\frac{d^2\hat{w}}{d\eta^2} + \left\{\frac{\partial[\ln\hat{\mu}_0]}{\partial\eta} - \frac{K}{[1-K\eta]} - \frac{\nu_\infty}{\nu_0}\hat{V}Re_\delta\right\}\frac{d\hat{w}}{d\eta} + \left\{\frac{B^2}{[1-K\eta]^2} - \frac{2K}{[1-K\eta]}\frac{\partial[\ln\hat{\mu}_0]}{\partial\eta} - \frac{4}{3}A^2 - \frac{\nu_\infty}{\nu_0}\frac{B\hat{U}Re_\delta}{[1-K\eta]}\right\}\hat{w} - \frac{AB}{3[1-K\eta]}\hat{u} + \left\{\frac{KA}{3[1-K\eta]} - A\frac{\partial[\ln\hat{\mu}_0]}{\partial\eta}\right\}\hat{v} - \frac{A}{3}\frac{d\hat{v}}{d\eta} = -\frac{\nu_\infty\rho_\infty}{\nu_0\rho_0}\frac{A\hat{p}Re_\delta}{2} \tag{14}$$

Single-underlined terms in the Eqs (11)–(14) are those retained both by Smith[3] and Kahawita and Meroney[2] while double underlining refers to the further curvature terms in K retained only by the latter authors. We follow these workers in neglecting terms involving K^2 and $(\delta/s)^2 B\eta\, d(s/r)/d\varepsilon$, which Smith's order-of-magnitude analysis showed were smaller than any other terms for his assumed ranges of variables. Present estimates which, in the light of predicted values of A, B and K, are based on smaller ranges of variables (Appendix 1), nevertheless confirm the above findings and indicate orders of magnitude for the second critical field reported below ranging from 10^4 to 10^{-6}; they also support Smith's argument for neglecting $(\delta/s)\, dB/d\varepsilon$ in all three momentum equations, and for limited binomial expansion of denominator terms in $[1-K\eta]$ to retain only linearity in K, the independent variable thereby conveniently treated as the eigenvalue. Although terms involving Re_δ often predominate, this, contrary to Smith's[3] assertion, is not always so; terms in A^2 may be at least comparable.

Of the terms in Eqs (11) to (14) not taken into account by Smith[3] and Kahawita and Meroney[2], the term:

$$\frac{\nu_\infty\delta Re_\delta}{\nu_0 s[1-K\eta]}\frac{\partial\hat{V}}{\partial\varepsilon}$$

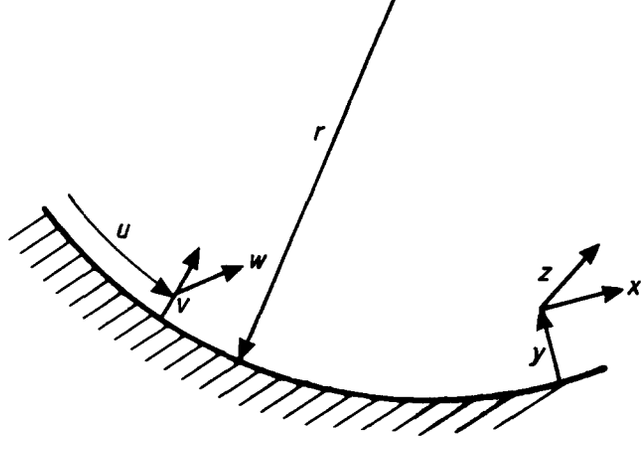

Fig 3 Orthogonal co-ordinate transformation for a concave surface

in Eq (13) can be between two and three orders of magnitude greater than the adjacent further curvature term $KB/[1-K\eta]^2$ included by Kahawita and Meroney. Moreover, neither they nor Smith include the terms $(A/3)\,d\hat{w}/d\eta$ in Eq (13) and $(A/3)\,d\hat{v}/d\eta$ in Eq (14), both of which can be greater than terms involving these same derivatives in Eqs (13) and (14) which were nevertheless retained by Smith[3] and Kahawita and Meroney[2]. These three omissions might help to account for differences between the stability predictions reported below and those of earlier treatments. Hall[15] also comments on the effects of the omissions from earlier analyses of various terms.

As already stated, the Gruschwitz[19] equations are used to evaluate the properties of the compressible laminar boundary layer. These are:

$$\frac{U_\infty\theta}{\nu_\alpha}\cdot\frac{d\theta}{dx}=F_1(k')-\frac{k}{d}[2-M_\infty^2F_2(k')] \tag{15}$$

$$d=\left[1+\left(\frac{\gamma-1}{2}\right)M_\infty^2\right]\left[\frac{1+M_\infty^2F_3(k')}{1+M_\infty^2F_4(k')}\right] \tag{16}$$

$$k'=\frac{\theta^2d}{\nu_\infty}\cdot\frac{dU_\infty}{dx}=\Lambda d \tag{17}$$

where F_1, F_2, F_3 and F_4 are universal functions of k'. In consequence, Gruschwitz[19] assumed the velocity distribution in the undisturbed laminar boundary layer to be:

$$\hat{U}=u_0/U_\infty=\left(2+\frac{\Lambda}{6}\right)\eta-\frac{\Lambda}{2}\eta^2+\left(\frac{\Lambda}{2}-2\right)\eta^3+\left(1-\frac{\Lambda}{6}\right)\eta^4 \tag{18}$$

which, for the case of Blasius flow considered here, reduces to:

$$\hat{U}=2\eta-2\eta^3+\eta^4 \tag{19}$$

and is adopted for both incompressible and compressible flow, together with the ratio of boundary-layer momentum thickness to boundary-layer thickness given by:

$$\frac{\theta}{\delta}=\frac{37}{315} \tag{20}$$

Since the concave surface is assumed adiabatic, its temperature is given by:

$$T_w=\left[1+\left(\frac{\gamma-1}{2}\right)Pr^{1/2}M_\infty^2\right]T_\infty \tag{21}$$

It is therefore reasonable to assume that within the boundary layer:

$$\hat{T}=\frac{T_0}{T_\infty}=\left(\frac{\rho_0}{\rho_\infty}\right)^{n-1}=\left(\frac{p_0}{p_\infty}\right)^{(n-1)/n}=1+\left(\frac{\gamma-1}{2}\right)Pr^{1/2}M_\infty^2(1-\hat{U}^2) \tag{22}$$

where n exceeds γ by an amount dependent on the loss of stagnation pressure relative to the radial static pressure change needed to balance the centrifugal force arising from surface curvature. For large curvatures and small losses in stagnation pressure, n may well approach γ, at least over part of the boundary layer, and since the effect on $(p_0/p_\infty)^{(n-1)/n}$ in Eq (22) is in any case small unless $n \gg \gamma$, n is assumed equal to γ, although it is accepted that conditions are not strictly isentropic. Variation of fluid properties with pressure is neglected. The representation of a number of terms in Eq (11)–(14) based on the foregoing will be found in Appendix 2.

To solve Eqs (11)–(14) by the Galerkin method we assume that:

$$\hat{u}=e^{-E\eta}[a_1\eta+a_2\eta^2+a_3\eta^3+a_4\eta^4+a_5\eta^5+a_6\eta^6] \tag{23}$$

$$\hat{v}=e^{-E\eta}[a_7\eta+a_8\eta^2+a_9\eta^3+a_{10}\eta^4+a_{11}\eta^5+a_{12}\eta^6] \tag{24}$$

$$\hat{w}=e^{-E\eta}[a_{13}\eta+a_{14}\eta^2+a_{15}\eta^3+a_{16}\eta^4+a_{17}\eta^5+a_{18}\eta^6] \tag{25}$$

$$\hat{p}=e^{-E\eta}[a_{19}\eta+a_{20}\eta^2+a_{21}\eta^3+a_{22}\eta^4+a_{23}\eta^5+a_{24}\eta^6] \tag{26}$$

where all a_i from $i=1$ to 24 are independent of η. As Smith[3] pointed out, six-term polynomials in η are needed because of the complexity and high order of Eqs (11) to (14). For instance, it can be shown by elimination that, for neutral stability ($B=0$) in incompressible flow, $\hat{v}$ is a sixth-order differential equation in η. The same is true for $\hat{u}$, $\hat{w}$ and $\hat{p}$. Eqs (23)–(26) automatically satisfy the boundary conditions that the disturbance must decay in the mainstream and that at the concave surface it must have zero values, ie:

$$\hat{u}(\infty)=\hat{v}(\infty)=\hat{w}(\infty)=\hat{p}(\infty)=0 \tag{27}$$

$$\hat{u}(0)=\hat{v}(0)=\hat{w}(0)=\hat{p}(0)=0 \tag{28}$$

Although we follow Smith's procedure[3] of introducing a decay factor E in the exponential terms in Eqs (23)–(26), Smith showed that its value is unimportant in the search for eigenvalues; numerical values of $\hat{u}$, $\hat{v}$, $\hat{w}$ and $\hat{p}$ are likewise unaffected, since a change in E is compensated by corresponding changes in a_i, from $i=1$ to 24.

After substitution of Eqs (23)–(26) in Eqs (11) to (14), the latter may be written in the form:

$$[P+QK]\{a_1, a_2, a_3, \ldots, a_{24}\}=[\omega_x, \omega_y, \omega_z, \omega_c] \tag{29}$$

where P and Q are square matrices whose elements are functions of η, { } represents a column matrix in the unknown coefficients, and ω_x, ω_y, ω_z and ω_c, which is also a column matrix, are the errors introduced in the differential equations due to the approximations in Eqs (23) to (26). Using the Galerkin method, Eq (29) may be transformed to give:

$$[P'+Q'K][a_1, a_2, a_3, \ldots, a_{24}]=[0, 0, 0, \ldots, 0] \tag{30}$$

where P' and Q' are square matrices of the coefficients obtained by the Galerkin equations. The coefficients of P' and Q' are evaluated by the Gauss–Laguerre formula; as before, the other matrices are column matrices. The twenty-four eigenvalues of Eq (30) are computed by the $Q-Z$ algorithm[26,27] at a value of ε determined by the selected value of Re_δ, increases in which allow downstream marching along the concave surface. If B is prescribed, the problem is to find the

least concave curvature, ie the smallest non-negative value of K, which will generate that degree of instability. According to convention, the solution is then expressed in terms of the least $G = Re_\theta(\theta/r)^{1/2}$ for given $\beta\theta Re_\theta$ over the possible range of $\alpha\theta$, where θ is related to δ by Eq (20).

The vortex energy used to help identify the relation between G and $\alpha\theta$ along a concave surface is defined as the total energy possessed by the disturbance. In the absence of Taylor–Goertler vorticity, the total energy is given by:

$$E_b = \iiint [\tfrac{1}{2}\rho_0(u_0^2+v_0^2)+p_0]\,dx\,dy\,dz \qquad (31)$$

while the total energy in the presence of vortices is:

$$E_a = \iiint [\tfrac{1}{2}\rho(u^2+v^2+w^2)+p]\,dx\,dy\,dz \qquad (32)$$

Vortex energy E_v is the difference between Eqs (31) and (32), and by substituting Eqs (1) to (5) into Eq (32) and neglecting as second order the cross terms which arise, this can be shown to be:

$$E_v = E_a - E_b = \int_0^\lambda \int_0^\infty \int_{x(\beta=0)}^x \left[\tfrac{1}{2}\rho(u_1^2+v_1^2+w_1^2)\cos^2\alpha z \exp\left(2\int \beta\,dx\right)\right] dx\,dy\,dz \qquad (33)$$

Since:

$$\int_0^{\lambda=2\pi/\alpha} \cos\alpha z\,dz = 0$$

and:

$$\int_0^{\lambda=2\pi/\alpha} \sin^2\alpha z\,dz = \int_0^{\lambda=2\pi/\alpha} \cos^2\alpha z\,dz \qquad (=\lambda/2)$$

Substitution of Eqs (23)–(25) into Eq (33) gives:

$$E_v = \int_0^\lambda \int_0^\infty \int_{x(\beta=0)}^x \left\{\tfrac{1}{2}\rho U_\infty^2 \exp(-2E\eta) \times[(a_1\eta\ldots a_6\eta^6)^2+(a_7\eta+\cdots+a_{12}\eta^6)^2 +(a_{13}\eta+\cdots+a_{18}\eta^6)^2] \times\cos^2\alpha z \exp\left(2\int_{x(\beta=0)}^x \beta\,dx\right)\right\} dx\,dy\,dz \qquad (34)$$

Since $\kappa = 1/r$ has been treated as the eigenvalue, the normalised values of a_i from $i=1$ to 18 multiplied by a constant n will also satisfy the system, but will not otherwise affect the integration. We therefore let $n=1$. Eq (34) is readily integrated with respect to z and also x if, as may be shown from its relation to β in Fig 7, the variation of $\exp(2\int_{x(\beta=0)}^x \beta\,dx)$ above unity is usually sufficiently small to be neglected in completing the integration with respect to x. On double integration it is in fact found for the data in Fig 7 that:

$$(x - x_{\beta=0}) \leqslant \int_{x(\beta=0)}^x \exp 2 \int_{x(\beta=0)}^x \beta\,dx\,dx \leqslant 1.4(x - x_{\beta=0}) \qquad (35)$$

The dimensionless vortex energy π_v can then be written:

$$\pi_v = \frac{4E_v}{\rho U_\infty^2 \lambda\delta(x-x_{\beta=0})} = \int_0^\infty \exp(-2E\eta)[(a_1\eta+\cdots+a_6\eta^6)^2 +(a_7\eta+\cdots+a_{12}\eta^6)^2 +(a_{13}\eta+\cdots+a_{18}\eta^6)^2]\,d\eta \qquad (36)$$

where the perturbed component of density ρ_1 has been taken outside the integration as being of second order compared to ρ_0. With $(\rho U_\infty^2\lambda\delta x) \propto (\theta Re_\theta^3)/(\alpha\theta)$, Eq (36) can be evaluated for given G and λ, from which β, and hence the corresponding values of a_i from $i=1$ to 18, can be obtained. From Eq (33) the vortex energy is clearly always greater than zero. We reiterate that the numerical value for E is unimportant in the search for eigenvalues, with numerical values for $\hat{u}$, $\hat{v}$, $\hat{w}$, $\hat{p}$ and vortex energies unaffected, because a change in E is compensated by corresponding changes in a_i from $i=1$ to $i=24$. This was verified by running the programme for a limited number of cases with E set equal to 1 and then 2.

Computations were carried out using double precision on the UWIST VAX computer for $2000 \leqslant Re_\delta \leqslant 6000$ (corresponding to $1.23\times10^5 \leqslant Re_x \leqslant 1.1\times10^6$), $0.2 < M_\infty < 0.9$, and stagnation conditions ranging from 1 bar to 15 bar, and 300 K to 1200 K. The average run time for a single eigenvalue was 3 min though some were longer. The accuracy of computations is assessed to be within 0.1%.

Discussion of predictions and comparison with measurements

Fig 4 shows, on logarithmic scales, the dependence of G on $\alpha\theta$ for the first critical field, with $\beta\theta Re_\theta$ as parameter. Although Fig 4 is for $Re_\delta = 2000$ and $M_\infty = 0.2$ at 1 bar and 300 K, it is almost indistinguishable from those for other conditions, as indeed are the illustrations which follow; within the quoted ranges, differences in G and $\alpha\theta$ values for given $\beta\theta Re_\theta$ are within 6 per cent. For $\beta\theta Re_\theta = 0.25$ these predictions agree substantially with those of Smith[3] and Kahawita and Meroney[2] but tend to larger G and leftward displacement of the minima as $\beta\theta Re_\theta$ increases. Thus for $\beta\theta Re_\theta = 5.0$, Smith's minimum G of 10 at $\alpha\theta = 0.65$ may be compared with our minimum G of 13 at $\alpha\theta = 0.38$. Correspondingly, the curve for $\beta\theta Re_\theta = 0$, into which those for all larger $\beta\theta Re_\theta$ merge, has for $G = 100$ a value for $\alpha\theta$ of 6.8 in Smith's case but only 5 in our case.

As G falls below unity, the neutral stability curve $\beta\theta Re_\theta = 0$ for the first critical state in Fig 4 departs from that of Smith to assume the asymptotic

form at $\alpha\theta = 0.3$ predicted (as shown in Fig 2) by Kahawita and Meroney[2] when they retained both normal flow and the additional curvature terms in their analysis. Under these conditions, Fig 4 also reproduces the cusp for minimum G reported by Kahawita and Meroney, but for $\beta\theta Re_\theta = 0.05$ and minimum G of 0.1 at $\alpha\theta = 0.15$ rather than their values of $\beta\theta Re_\theta = 0.11$ and minimum G of 0.16 at $\alpha\theta = 0.12$. Although these differences may well be attributable to the neglect by Kahawita and Meroney of apparently important terms in the analysis, as discussed in the previous section, there is sufficient agreement to support the suggestion of Chang and Sartory[14] that at lower $\alpha\theta$ (and small $\beta\theta Re_\theta$), Smith's predictions of G for the first critical field are too large, but to dispute the conclusion of Kahawita and Meroney that the Galerkin method used here and previously by Smith in conjunction with the same exponential decay rate contributed to the discrepancy between his predictions and their own. (Hall[15] attributes discrepancies at low $\alpha\theta$ to non-applicability of parallel flow theory, which in essence is what is suggested above).

Whatever the reason for that discrepancy, there is strong evidence that the normal flow terms determine the asymptotic form of the first critical state at $\alpha\theta = 0.3$ in Fig 4. Our analysis also confirms the assertion of Kahawita and Meroney that eigenvalues of K to give $G < 0.1$ for neutral stability at $\alpha\theta$ below 0.3 do not exist. Nor was it possible in this region to obtain amplification curves in the range $0.05 > \beta\theta Re_\theta > 0$. It is concluded that the influence of the normal velocity and additional curvature terms steadily increases as $\beta\theta Re_\theta$ falls below about 0.25 but above this value their effects are marginal.

Also shown in Fig 4 are contours of dimensionless vortex energy π_v. The vortex energy E_v, which evidently derives from mainstream kinetic energy either directly or through the boundary layer, is used to calculate π_v with a view to providing an additional criterion to help determine vortex development for given conditions, ie to determine λ by establishing the relation between G and $\alpha\theta$. While its numerical variation is small, the locus of minimum π_v, which lies between that of minimum G for given $\beta\theta Re_\theta$ and the first neutral stability curve, tends to a slope of 1.5, which implies constant wavelength, as it approaches the least possible value of 3.6×10^{-3}. This corresponds to $\alpha\theta = 0.68$, $G = 5.3$ and $\beta\theta Re_\theta = 1.6$. Were vortex development along a concave surface to follow the locus of minimum π_v, as seems not unreasonable, its further amplification to greater G would involve an increase in dimensionless vortex energy, and leaving unresolved the value of $\alpha\theta$ (and G) at which the instability originated, unless at low G the locus of minimum π_v merged with the neutral stability asymptote. As is evident from Fig 4, this would imply an inverse relationship between G and $\alpha\theta$ no matter what the value of G at which merging occurred. This conflicts with experimental evidence, to be discussed below, that λ remains substantially constant.

The alternative is that instability may be initiated at $\alpha\theta$ below 0.3 but, as noted by Kahawita and Meroney, it raises the question of the physical significance of zero G for neutral stability and the improbability of its incidence at zero x. Meksyn's identification[1] of more than one critical state led the authors to search for eigenvalues yielding much higher values

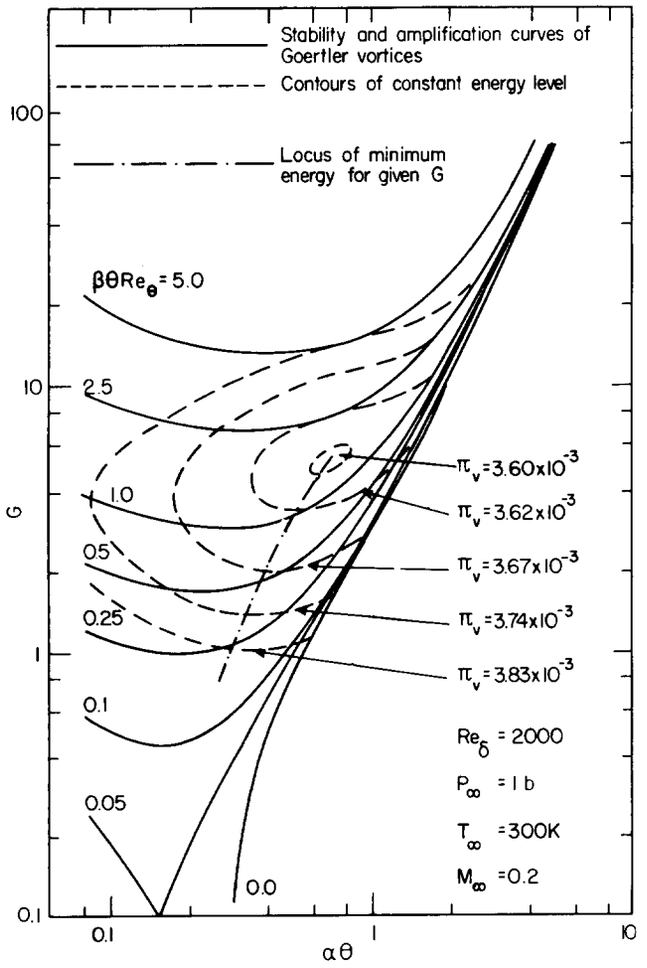

Fig 4 Predictions for the first critical field (I) including contours of dimensionless vortex energy

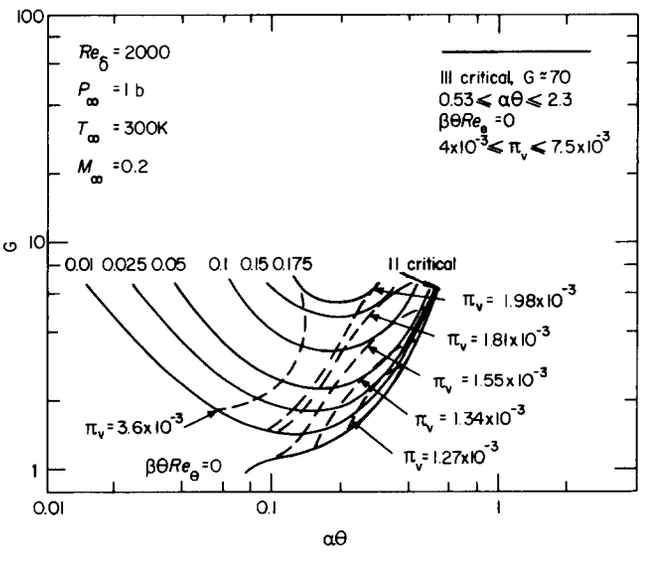

Fig 5 Predictions for the second (II) and third (III) critical fields including contours of dimensionless vortex energy

of least G for neutral stability than had been examined for $\alpha\theta < 0.3$ in Fig 4.

The results are presented in Fig 5. The neutral stability curve for the second critical state covers only a limited range of $\alpha\theta$ between 0.074, when $G = 0.97$, and 0.53, when $G = 6.65$. For marginal stability no eigenvalues could be found for $\alpha\theta < 0.074$ and though the range of $\alpha\theta$ thus extends below 0.3, overall it is much less than that of the first critical state. Amplification values of $\beta\theta Re_\theta$ up to 0.175 are also less than for the first critical field but the curves similarly extend outside the range of $\alpha\theta$ for neutral stability, to values as low as 0.015. As with the first critical state, the second neutral stability curve with $\beta\theta Re_\theta = 0$ merges with those of greater $\beta\theta Re_\theta$ at high $\alpha\theta$ and is also like the first in alone having no mathematical minimum. The least G for neutral stability of 0.97 may nevertheless be compared with Smith's[3] minimum G of 0.31 and Meksyn's[1] minimum G of 3.65, both for the first critical state, and Meksyn's minimum of 10.7 for the second critical state.

Although much of the field for the second critical state lies within that of the first in Fig 4, Fig 5 shows the second to have an upper limit for G of about 7 for $0.175 \geqslant \beta\theta Re_\theta \geqslant 0.01$. Attempts to find eigenvalues yielding higher least G for $\alpha\theta$ below 0.53 were unsuccessful. In the range $0.53 \leqslant \alpha\theta \leqslant 2.3$ eigenvalues were however found, but in all cases only for $\beta\theta Re_\theta = 0$. These yielded a uniform least G of 70 (Fig 5). No other eigenvalues could be found for what is thought to be a third critical state, and which in terms of G is separated from the second by an order of magnitude.

Martin and Brown[8] note that Liepmann's[4,5] laminar boundary-layer measurements on concave surfaces in zero pressure gradient show transition to turbulence to begin if G exceeds 7. These measurements were made at low U'_∞/U_∞. Although Dryden[25] states that G for transition may be as high as 9 for very low mainstream turbulence intensities, in zero pressure gradient it is inconceivable that it could be as much as 70. Against this experimental evidence, the absence of eigenvalues giving least G above 7 for $0.015 < \alpha\theta < 0.53$ suggests that in this range either the assumed form of the disturbances in Eqs (1)–(5) in conjunction with Eqs (23)–(26) no longer holds, or the laminar boundary-layer equations on which the analysis is based become invalid, because the flow ceases to be laminar. (In this context Hall[16] showed that for a limited choice of boundary layer velocity profiles, the distribution at least influences the neutral curves). If this is so, the calculations would appear to predict the onset of transition on concave surfaces when mainstream turbulence is negligible. Without measurements at $G = 70$, it is impossible to say whether the third critical state for $0.53 \leqslant \alpha\theta \leqslant 2.3$ has physical significance, though it would seem unlikely. Although the present treatment does not take into account the influence of U'_∞/U_∞, it is of interest that the G range for the second critical field encompasses the experimental transition range between 2.3 and 6.1 determined by Brown and Martin[9] for turbine blade pressure surfaces in cascades and turbulence intensities up to 0.17 in favourable pressure gradients below the laminarisation value of k.

If it is accepted that vortex initiation in laminar boundary-layer flow along concave surfaces is governed by the second critical state rather than the first, at least for $\alpha\theta \leqslant 0.3$ (when $G \leqslant 2.0$), the least G and $\alpha\theta$ for neutral stability are 0.97 and 0.074 respectively. The case is strengthened by the contours of constant π_v in Fig 5 which, like those of the first critical field, for given G diminish in value (although more rapidly) as $\alpha\theta$ increases; most striking are the numerical values of dimensionless vortex energy, roughly half those in Fig 4 except for $\pi_v = 3.6 \times 10^{-3}$, which minimum for the first critical field is included to emphasise the comparison. Unlike the first, the second critical field has no locus of minimum π_v, only a singular minimum value of 1.25×10^{-3} on the neutral stability curve at $G = 2.0$, $\alpha\theta = 0.3$.

The concept of least dimensionless vortex energy thus favours the second critical state over the first and, as may be seen by comparing the value of π_v for the (supposed) third critical state in Fig 5, it also favours the second over the third. The effect of applying the least energy criterion seems to be to narrow still further the possible range of $\alpha\theta$ for vortex inception along the neutral stability curve for the second critical state to values from 0.074 to 0.3, when dimensionless vortex energy is least; it may be more than coincidence that this is also the asymptotic value of $\alpha\theta$ for the first critical state.

It is also significant that π_v contours for 1.98×10^{-3} and 1.81×10^{-3}, and, to a lesser extent, those for lower values in Fig 5, follow fairly closely the relation $G/(\alpha\theta)^{1.5} =$ constant for uniform λ. As is seen in Fig 6, where the measurements of Tani[11], Tani and Sakagami[12] and Yeo[22] for the Blasius flow of air and Winoto and Crane[21] for water flow in a curved channel, are superimposed on the second critical field, the tendency for vortex development to take place at constant wavelength is strong. Also shown in Fig 6 are the Blasius flow measurements for air of Bippes and Goertler[23] and Han and Cox[24], based, like others in Fig 6, (save those of Winoto and Crane[21] which are derived from measured θ) on Eq (20) and $\delta/x =$

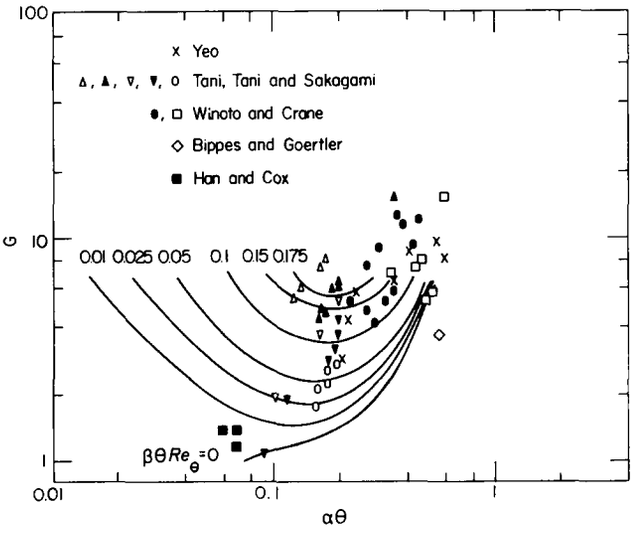

Fig 6 Comparison of measurements with predictions for the second critical field

$4.64 \times Re_x^{-1/2}$. The values plotted differ somewhat from those presented by the above authors, the bases of whose calculations of θ, and hence G, being unfortunately not clear from their papers. Apart from the single data point of Bippes and Goertler, of marginally larger $\alpha\theta$ than the second neutral stability curve, the location of the above measurements further supports the arguments favouring the second critical field; none has G values below the second neutral stability curve, though one is on it at $\alpha\theta = 0.09$. Comparison of Figs 5 and 6 shows measurements, which unfortunately do not include reliable assessments of amplification rate, to be concentrated in the region of relatively low π_v, only one approaching $\pi_v = 3.6 \times 10^{-3}$. Those with values of $G > 7$ appear to lie in a non-laminar region (which might well be a transition region), one such having been confirmed by Crane[28]. The counter argument that G values above 7 merely imply a laminar reversion to the first critical field also implies a step increase in β of more than an order of magnitude, which from an experimental standpoint seems unlikely. If minimum π_v rather than minimum K had been the criterion for the selection of the critical state, the second critical field would become the first, and vice versa. Perhaps the analysis is then more clearly seen as an eigenvalue problem with multiple solutions, typical of almost any physical problem with homogeneous boundary conditions like Eqs (27) and (28).

While vortex energy considerations therefore seem to limit the possible range of vortex wavelengths, other as yet unidentified influences appear finally to determine λ for given initial conditions. Thus Tani's measurements, each set at virtually constant wavelength, can be correlated by the equation:

$$\frac{U_\infty r}{\nu_\infty} \frac{1}{(\alpha r)^{1.5}} = \frac{114 U_\infty^{0.92}}{r^{1.41}} \tag{37}$$

over the ranges $16 \geq U_\infty \geq 3$ and $10 \geq r \geq 5$, where U_∞ is in m/s and r in m. Wavelength is then nearly independent of mainstream velocity and

$$r\lambda^{3/2} \simeq \text{constant} \tag{38}$$

which suggests that wavelength is finally determined by radius of curvature.

Successive increases in $\beta\theta Re_\theta$ during vortex development along a concave surface at constant λ do not necessarily involve corresponding increases in the amplification rate β. Fig 7 depicts β as a function of x (both made dimensionless by reference only to initial conditions) with dimensionless wavelength λ as a parameter; this is for the second field predicted in Fig 5. For all λ the amplification rate initially increases with x but subsequently diminishes after reaching a maximum determined by λ. The greatest possible value of $\beta(\nu_\infty r^2/U_\infty)^{1/3}$ of about 0.02 is achieved for a wavelength corresponding to vortex initiation at the least possible value of G of 0.97 on the second neutral stability curve, such that $G/(\alpha\theta)^{3/2} = 48.2$ and $\lambda[U_\infty^2/(\nu_\infty^2 r)]^{1/3} = 83.2$. This is well within the range of Tani's[11] measurements (Fig 6). Maximum values of $\beta\,(\nu_\infty r^2/U_\infty)^{1/3}$ for smaller and larger dimensionless wavelengths are less than 0.02. Fig 7 also shows the upper boundary of the second critical field, corresponding to the upper limits for G.

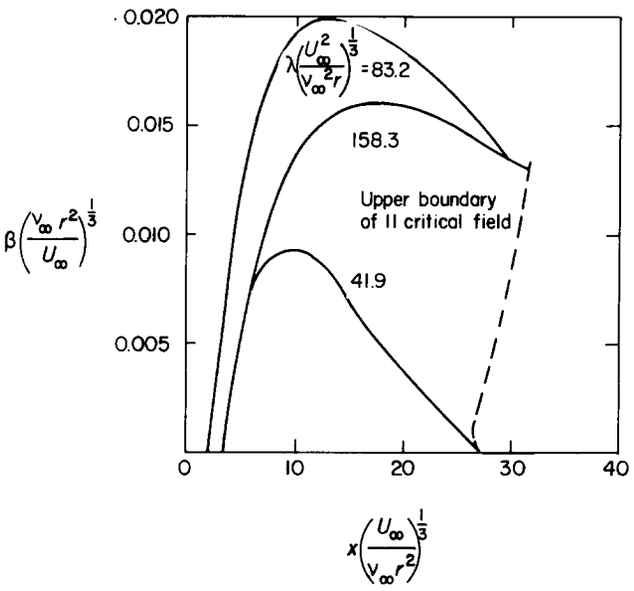

Fig 7 Predicted amplification rate for the second critical field as a function of surface distance for various vortex wavelengths, all in dimensionless terms

Figs 8–10 portray the normalised perturbed velocity components as functions of η predicted for $\alpha\theta = 0.117$ and three values of $\beta\theta Re_\theta$, viz 0, 0.05 and 0.1, for the second critical field. These are typical in that $\hat{u}$, $\hat{v}$ and $\hat{w}$, while unequal in magnitude, are nevertheless of the same order; all three compare favourably with those of Smith[3], albeit for the first critical field, in extending to five or six boundary-layer thicknesses, and well illustrate the toroidal nature of

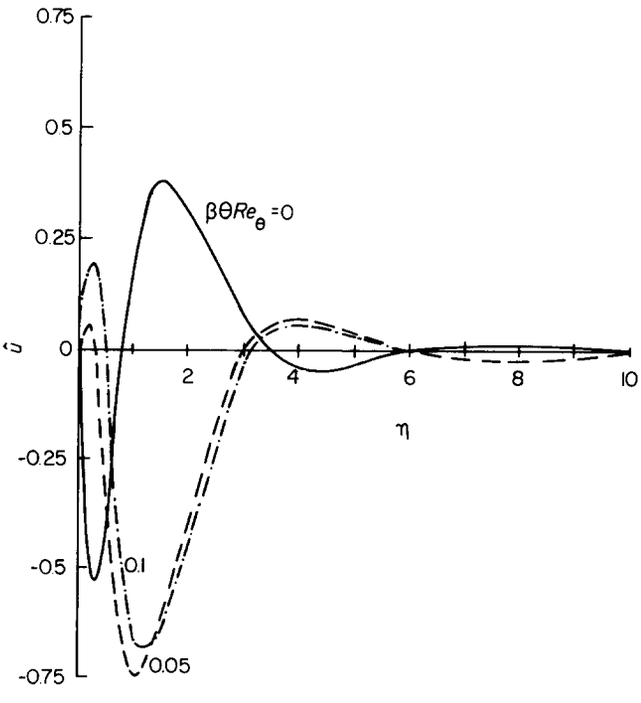

Fig 8 Perturbed normalised velocity component in the x-direction relative to dimensionless distance from concave surface for II critical

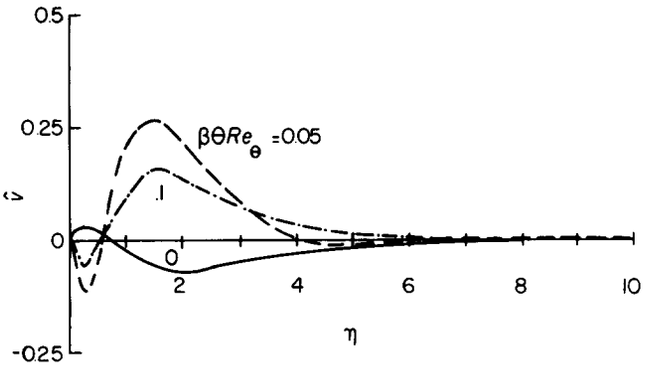

Fig 9 Perturbed normalised velocity component in the y-direction relative to dimensionless distance from concave surface for II critical

Taylor–Goertler vortices. Unfortunately there appear to be no reliable measurements of $\hat{u}$, $\hat{v}$ and $\hat{w}$ with which comparisons can be made.

Conclusions

In the analysis presented here, the Galerkin method is used to study the stability of Taylor–Goertler vortices induced in the flow of a laminar boundary-layer with uniform mainstream velocity along a concave surface. The analysis, which includes terms in the continuity and momentum equations neglected in earlier theoretical treatments, indicates the existence of more than one critical state, as previously predicted by Meksyn[1] but at generally lower values of Goertler number.

Predictions for the first critical field are in good accord at higher G with those of Smith[3] and Kahawita and Meroney[2], and at lower G with the neutral stability asymptote of the latter authors at $\alpha\theta = 0.3$ when they retained normal flow terms in their analysis. Neutral stability at lower $\alpha\theta$ is found to occur only for the second critical state, whose amplification field over the limited range of G between 0.97 and 7 corresponds well with the range of available measurements, almost all of which imply vortex development

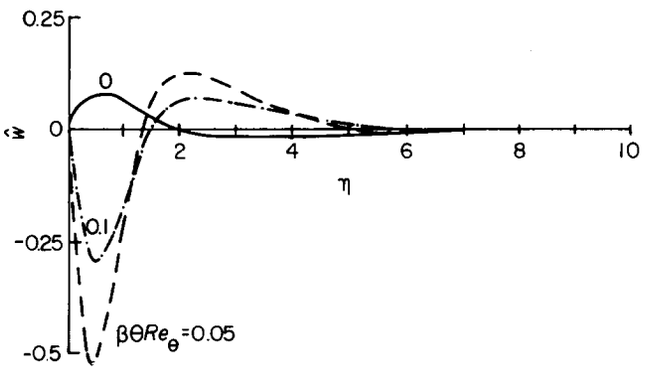

Fig 10 Perturbed normalised velocity component in the z-direction relative to dimensionless distance from concave surface for II critical

at virtually constant wavelength; those of Liepmann[4,5] also indicate a transition to turbulence if G exceeds the limiting predicted value of 7 for the second critical state. For laminar flow, this would appear to invalidate the third critical state identified for G of about 70 and $\alpha\theta > 0.53$.

The second critical field appreciably narrows the possible range of vortex wavelengths and further persuasive evidence in its favour is provided by consideration of dimensionless vortex energy levels. Over the range of available measurements, those for the second critical field are half those of the first and considerably less than for the third, thus supporting the concept of least dimensionless vortex energy as an influential factor in the behaviour of three-dimensional disturbances. The other influences which help determine vortex wavelength remain to be identified.

Our predictions are found to apply to stagnation conditions up to 15 bar and 1200 K, mainstream Mach numbers up to 0.9 and Reynolds numbers, based on boundary-layer thickness, between 2000 and 6000.

Acknowledgements

The authors would like to acknowledge the extensive computing support given by UWIST and its financial support to one of us (KHY).

References

1. **Meksyn D.** Stability of viscous flow over concave cylindrical surfaces. *Proc. Roy. Soc. Lond. 1950, A***203**, *253–265*
2. **Kahawita R. and Meroney R.** The influence of heating on the stability of laminar boundary layers along concave curved walls. *ASME J. Appl. Mech. 1977,* **44**, *11–17*
3. **Smith A. M. O.** On the growth of Taylor–Goertler vortices along highly-concave walls. *Quart. Appl. Maths. 1955,* **8**, *233–262*
4. **Liepmann H. W.** Investigations on laminar boundary-layer stability and transition on curved boundaries. *NACA Wartime Rep. 1943, W-107*
5. **Liepmann H. W.** Investigation of boundary-layer transition on concave walls. *NACA Wartime Rep. 1945, W-87*
6. **Goertler H.** Uber eine dreidimensionale instabilität laminarer grenzschlichten an konkaven wänden. *Nachr. Wiss. Ges. Göttingen, Math. Phys. Klasse., 1940, Abt 2, 1–26*
7. **McCormack P. D., Welker H. and Kelleher M.** Taylor–Goertler vortices and their effect on heat transfer. *ASME J. Heat Transfer, 1970,* **92**, *101–112*
8. **Martin B. W. and Brown A.** Factors influencing heat transfer to the pressure surfaces of gas turbine blades. *Int. J. Heat and Fluid Flow, 1979,* **1**, *107–114*
9. **Brown A. and Martin B. W.** Flow transition phenomena and heat transfer over the pressure surfaces of gas turbine blades. *ASME J. Engng. for Power, 1982,* **104**, *360–367*
10. **Launder B.** Laminarization of the turbulent boundary-layer in a severe acceleration. *ASME J. Appl. Mech. 1964,* **31**, *707–708*
11. **Tani I.** Production of longitudinal vortices in the boundary layer along a concave wall *J. Geophysical. Res. 1962,* **67**, *3075–3080*
12. **Tani I and Sakagami J.** Boundary-layer instability at subsonic speeds *J. Proc. Int. Council Aero Sci. Third Congress, 1962, 391–403*

13. **Hammerlin G.** Uber das eigenwertproblem dreidimensionalen instabilität laminarer grenzschichten längs konkaven wänden. *J. Ratl. Mech. Anal. 1955*, **4**, *279–321*

14. **Chang T. S. and Sartory W. K.** Hydromagnetic Goertler instability in a boundary layer on a concave wall. *Developments in theoretical and applied mechanics*, **4**, *ed. D. Frederick, 1968*

15. **Hall P.** Taylor–Gortler vortices in fully developed or boundary-layer flows: linear theory. *J. Fluid. Mech., 1982*, **124**, *475–494*

16. **Hall P.** The linear development of Goertler vortices in growing boundary-layers, *J. Fluid Mech. 1983*, **130**, *41–58*

17. **Aihara Y.** Stability of the compressible boundary-layer along a curved wall under Goertler-type disturbances. *Tokyo University, Aeronautical Research Institute, 1961, Rep. 362, 31–37*

18. **Kobayashi R. and Kohama Y.** Taylor–Goertler instability of laminar compressible boundary layers. *AIAA Journal, 1977*, **15**, *1723–1727*

19. **Gruschwitz E.** Calcul approché de la couche limite laminaire en ecoulement compressible sur un paroi non-conductrice de la chaleur. *ONERA Publication, 1950*, **47**, *Paris*

20. **Yeo K. H.** *Personal communication, 1980*

21. **Winoto S. H. and Crane R. I.** Vortex structures in laminar boundary layers on a concave wall. *Int. J. Heat and Fluid Flow, 1980*, **2**, *221–231*

22. **Yeo K. H.** *Ph.D. Thesis, University of Wales, 1982*

23. **Bippes H. and Goertler H.** Dreidimensionale Störungen in der Grenzschicht an einer konkaven wand. *Acta Mechanica, 1972*, **14**, *251–267*

24. **Han L. S. and Cox W. R.** A visual study of turbine blade pressure-side boundary layers, *ASME Paper No 82-GT-47, 1982*

25. **Dryden W. L.** Recent advances in the mechanics of boundary-layer flow. *Advances in applied mechanics, Part I, ed. R. von. Mises and Th. von Karman, New York, 1–40, 1948*

26. **Moler C. B. and Stewart G. W.** An algorithm for generalised matrix eigenproblems. *Siam. J. Numer. Analysis, 1973*, **10**, *241–256*

27. **Ward R. C.** An extension of the *Q–Z* algorithm for solving the generalised matrix eigenvalue problem. *NASA Tech. Note 1973, D-7305*

28. **Crane R. I.** *Personal communication, 1982*

Appendix 1 Estimated order-of-magnitude of terms in Eqs (11)–(14)

The procedure adopted by Smith[3] was to attempt to assess, in advance of his analysis, likely orders of magnitude of the terms in the continuity and momentum equations with a view to determining which might subsequently be safely neglected. In Eqs (11)–(14) far fewer terms are neglected, and orders of magnitude have been estimated after completion of the analysis from the computer predictions, based as stated on Blasius flow of air at stagnation conditions of from 1 bar to 15 bar and 300 K to 1200 K, $0.2 \leqslant M_\infty \leqslant 0.9$ and $2000 \leqslant Re_\delta \leqslant 6000$, together with Eqs (19), (20) and (22) and their derivatives. In view of the conclusions drawn from the analysis, orders of magnitude relate only to predictions for the second critical field. As is seen in Fig. 5, these cover the ranges $0.97 \leqslant G \leqslant 7.0$, $0 \leqslant \beta\theta Re_\theta \leqslant 0.175$ and $0.015 \leqslant \alpha\theta \leqslant 0.53$, although for marginal stability ($\beta\theta Re_\theta = 0$) the wavenumber range is restricted to $0.074 \leqslant \alpha\theta \leqslant 0.53$. Since measurements indicate that $\alpha\theta$ never diminishes with increasing G and $\beta\theta Re_\theta$, orders of magnitude are assessed for that range of $\alpha\theta$. These calculations are presented below in tabular form.

Variable	*Minimum value*	*Maximum value*
A	0.63	4.51
B	0	6.34×10^{-3}
K	1.61×10^{-5}	7.55×10^{-3}
Re_θ	235	704.8
Re_δ	2000	6000
$\hat{U}$	0	1
$\mathrm{d}\hat{U}/\mathrm{d}\eta$	0	2
$\hat{U}Re_\delta$	0	6000
$Re_\delta\,\mathrm{d}\hat{U}/\mathrm{d}\eta$	0	12000
$\hat{V}Re_\delta$	0	4.33
$Re_\delta\partial\hat{V}/\partial\eta$	0	7.28
$(\delta/s)Re_\delta\partial\hat{V}/\partial\varepsilon$	0	7.5×10^{-2}
$(\delta/s)\,\mathrm{d}B/\mathrm{d}\varepsilon$	1.4×10^{-5}	2.77×10^{-5}
s/r	2.97×10^{-3}	4.17
$\mathrm{d}(s/r)/\mathrm{d}\varepsilon$	0	56.3
$(\delta/s)^2B\eta\,\mathrm{d}(s/r)/\mathrm{d}\varepsilon$	0	1.17×10^{-6}

Appendix 2 Representation of terms in Eqs (11)–(14)

Given that the characteristic equation of state for a perfect gas is valid for both undisturbed and disturbed flow, it follows from Eqs (4) and (5) that:

$$p_0 = \rho_0 RT_0 \qquad p_1 = \rho_1 RT_0 \tag{A1}$$

and hence from Eqs (9) and (10) that:

$$\hat{p} = p_1/(\tfrac{1}{2}\rho_\infty U_\infty^2) = \rho_1 RT_0/(\tfrac{1}{2}\rho_\infty U_\infty^2) = \hat{\rho}RT_0/(\tfrac{1}{2}U_\infty^2) \tag{A2}$$

Since for compressible flow:

$$U_\infty^2 = M_\infty^2 \gamma RT_\infty \tag{A3}$$

we have between Eqs (A2) and (A3):

$$\hat{\rho} = \frac{\gamma M_\infty^2 \hat{p}}{2\hat{T}} \tag{A4}$$

and in Eqs (11)–(14) we can therefore from Eq (A7) substitute as follows:

$$\frac{\hat{\rho}}{\hat{\rho}_0} = \frac{\gamma M_\infty^2 \hat{p}}{2\hat{\rho}_0\hat{T}} \qquad \frac{1}{\hat{\rho}_0}\frac{\partial\hat{\rho}}{\partial\eta} = \frac{\gamma M_\infty^2}{2\hat{\rho}_0\hat{T}}\frac{\partial\hat{p}}{\partial\eta} \tag{A5}$$

Differentiation of Eq (22) gives:

$$\frac{\partial\hat{T}}{\partial\eta} = \frac{\partial}{\partial\eta}\left(\frac{T_0}{T_\infty}\right) = -(\gamma-1)Pr^{1/2}M_\infty^2\hat{U}\frac{\partial\hat{U}}{\partial\eta} \tag{A6}$$

and since, from Eqs (10) and (A1):

$$\frac{p_0}{p_\infty} = \hat{p}_0 = \frac{\rho_0 T_0}{\rho_\infty T_\infty} = \hat{\rho}_0\hat{T} \tag{A7}$$

it follows that:

$$\frac{\partial\hat{\rho}_0}{\partial\hat{T}} = -\frac{\hat{\rho}_0}{\hat{T}} \qquad \frac{1}{\hat{\rho}_0}\frac{\partial\hat{\rho}_0}{\partial\eta} = \frac{1}{\hat{\rho}_0}\frac{\partial\hat{\rho}_0}{\partial\hat{T}}\frac{\partial\hat{T}}{\partial\eta} \tag{A8}$$

By combination of Eqs (A6) and (A8) we can substitute in Eqs (11)–(14) as follows:

$$\frac{\partial}{\partial\eta}[\ln\hat{\rho}_0] = \frac{1}{\hat{\rho}_0}\frac{\partial\hat{\rho}_0}{\partial\eta} = (\gamma-1)Pr^{1/2}M_\infty^2\frac{\hat{U}}{\hat{T}}\frac{\partial\hat{U}}{\partial\eta} \tag{A9}$$

where $\hat{U}$ and $\hat{T}$ are defined by Eqs (19) and (22) respectively. Since we have assumed in Eq (6) that:

$$\mu_0 \propto T_0^{3/2}/(T_0+114)$$

it follows that:

$$\frac{1}{\mu_0}\frac{\mathrm{d}\mu_0}{\mathrm{d}T_0}=\frac{1}{T_0}\left[\frac{3}{2}-\frac{T_0}{(T_0+114)}\right] \tag{A10}$$

or:

$$\frac{1}{\hat{\mu}_0}\frac{\mathrm{d}\hat{\mu}_0}{\mathrm{d}\hat{T}}=\frac{1}{\hat{T}}\left[\frac{3}{2}-\frac{T_0}{(T_0+114)}\right] \tag{A11}$$

Eq (A6) with Eq (A11) then yields the following substitution in Eqs (11)–(14):

$$\begin{aligned}\frac{\partial}{\partial\eta}[\ln\hat{\mu}_0]&=\frac{1}{\hat{\mu}_0}\frac{\partial\hat{\mu}_0}{\partial\eta}=\frac{1}{\hat{\mu}_0}\frac{\mathrm{d}\hat{\mu}_0}{\mathrm{d}\hat{T}_0}\frac{\partial\hat{T}_0}{\partial\eta}\\&=-\left[\frac{3}{2}-\frac{T_0}{(T_0+114)}\right]\\&\quad\times(\gamma-1)Pr^{1/2}M_\infty^2\frac{\hat{U}}{\hat{T}}\frac{\partial\hat{U}}{\partial\eta}\end{aligned} \tag{A12}$$

The steady-flow continuity equation for flow along a concave surface, which is:

$$\frac{\partial}{\partial x}(\rho_0 u_0)+\frac{\partial}{\partial y}(\rho_0 v_0)=0 \tag{A13}$$

implies a stream function ψ such that:

$$\frac{\partial\psi}{\partial x}=-\frac{\rho_0 v_0}{\rho_\infty}=-\frac{\rho_0\hat{V}U_\infty}{\rho_\infty} \tag{A14}$$

$$\frac{\partial\psi}{\partial y}=\frac{\rho_0 u_0}{\rho_\infty}=\frac{\rho_0\hat{U}U_\infty}{\rho_\infty} \tag{A15}$$

Integration of (A15) gives in combination with Eq (22)

$$\begin{aligned}\psi&=\int\frac{\rho_0}{\rho_\infty}u_0\,\mathrm{d}y\\&=U_\infty\delta\int\left[1+\left(\frac{\gamma-1}{2}\right)\right.\\&\quad\left.\times Pr^{1/2}M_\infty^2(1-\hat{U}^2)\right]^{1/(\gamma-1)}\hat{U}\,\mathrm{d}\eta\end{aligned} \tag{A16}$$

Substitution for $\hat{U}$ from Eq (19) permits completion of the integration of Eq (A16) by Gauss–Legendre quadrative procedure. With Eqs (22) and (A16), Eq (A14) then gives the following for substitution in Eqs (11) to (14):

$$\hat{V}=-\frac{1}{U_\infty}\left[1+\left(\frac{\gamma-1}{2}\right)Pr^{1/2}M_\infty^2(1-\hat{U}^2)\right]^{-1/(\gamma-1)}\frac{\partial\psi}{\partial x} \tag{A17}$$

$$\begin{aligned}\frac{\partial\hat{V}}{\partial\eta}&=-\frac{1}{U_\infty}\left\{\left[1+\left(\frac{\gamma-1}{2}\right)Pr^{1/2}M_\infty^2(1-\hat{U}^2)\right]^{-\gamma/(\gamma-1)}\right.\\&\quad\times Pr^{1/2}M_\infty^2\hat{U}\frac{\partial\hat{U}}{\partial\eta}\frac{\partial\psi}{\partial x}\\&\quad+\left[1+\left(\frac{\gamma-1}{2}\right)Pr^{1/2}M_\infty^2(1-\hat{U}^2)\right]^{-1/(\gamma-1)}\\&\quad\left.\times\frac{\partial^2\psi}{\partial x\,\partial\eta}\right\}\end{aligned} \tag{A18}$$

$$\begin{aligned}\frac{1}{s}\frac{\partial[U_\infty\hat{V}]}{\partial\varepsilon}&=\frac{\partial v_0}{\partial x}=-\frac{\rho_\infty}{\rho_0}\frac{\partial^2\psi}{\partial x^2}\\&=-\left[1+\left(\frac{\gamma-1}{2}\right)Pr^{1/2}M_\infty^2(1-\hat{U}^2)\right]^{-1/(\gamma-1)}\frac{\partial^2\psi}{\partial x^2}\end{aligned} \tag{A19}$$